Investigation of 3-(1,3-oxazol-5-yl)aniline as a highly efficient corrosion inhibitor for mild steel in 1 M HCl solution

Ahmed Alamiery[1,2,*,†] and Waleed K. Al-Azzawi[3]

[1]*Department of Chemical and Process Engineering, Faculty of Engineering and Built Environment, University Kebangsaan Malaysia (UKM), Bangi P.O. Box 43000, Selangor, Malaysia;* [2]*Energy and Renewable Energies Technology Center, University of Technology, Baghdad 10001, Iraq;* [3]*Al-Farahidi University, Baghdad 10001, Iraq*

Abstract

Mild steel corrosion in acidic environments presents a significant challenge with detrimental consequences for both industrial infrastructure and the environment. Effective corrosion control measures are crucial to prolonging the lifespan of equipment. Inhibition techniques have proven to be an efficient method for protecting mild steel from corrosion, particularly in acidic conditions. This study investigates the efficacy of 3-(1,3-oxazol-5-yl)aniline (3-OYA) as a corrosion inhibitor for mild steel in a hydrochloric acid (HCl) solution. Traditional weight-loss tests, as well as electrochemical techniques, such as potentiodynamic polarization and electrochemical impedance spectroscopy, were employed to evaluate the corrosion inhibition performance. The results reveal that 3-OYA, at a concentration of 0.05 mM, exhibits an outstanding protection efficacy of 93.5%. This remarkable performance can be attributed to the formation of a protective adsorption layer on the mild steel surface, effectively inhibiting the corrosion rate and enhancing inhibitory efficacy. The inhibition efficiency was found to increase with increasing inhibitor concentration, while it decreased with rising temperature. Langmuir adsorption isotherm analysis confirmed the high adsorption–inhibition activity of 3-OYA. The ΔG^{o}_{ads} value indicated the occurrence of both physical and chemical adsorption mechanisms on the mild steel surface. Furthermore, density functional theory (DFT) calculations were utilized to determine the quantum chemical parameters and establish a correlation between the inhibition activity and the molecular structure. The consistency between the experimental and theoretical analyses reinforces the robustness of our findings.

Keywords: corrosion inhibitor; mild steel; oxazol; aniline; DFT; HOMO

*Corresponding author:
dr.ahmed1975@gmail.com
or
dr.ahmed1975@ukm.edu.my

Received 15 April 2023; revised 26 May 2023; accepted 21 June 2023

1 INTRODUCTION

Mild steel, also known as plain-carbon steel, low-carbon steel, carbon steel or A36 carbon steel, is widely utilized in various industries due to its availability, physical properties and cost-effectiveness [1–7]. However, when exposed to acidic solutions used in processes, such as acid de-scaling, oil well acidizing, acid pickling, petrochemical processes and industrial cleaning, mild steel experiences significant corrosion, leading to substantial financial losses [8]. To address this issue, corrosion inhibitors are employed, which can be categorized as inorganic or organic compounds. While inorganic inhibitors exhibit either anodic or cathodic actions, organic inhibitors possess dual actions and can form protective films through adsorption [9–11]. Organic corrosion inhibitors are often more cost-effective and efficient compared to their inorganic counterparts [12]. In the realm of organic corrosion inhibitors, several classes of compounds, including aromatic α,β-unsaturated aldehydes, acetylenic alcohols, α-alkenyl phenones, quaternary ammonium compounds, amines, carbonyl-containing inhibitors obtained through condensation reactions and nitrogen- or sulfur-containing compounds, have demonstrated effectiveness in acidic environments [15–22].

†, https://orcid.org/0000-0003-1033-4904

International Journal of Low-Carbon Technologies 2023, 18, 850–862

https://doi.org/10.1093/ijlct/ctad069 Advance Access publication 29 July 2023

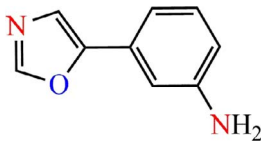

Figure 1. *3-OYA (a) chemical and (b) optimized structures.*

Acetylenic alcohols, known for their high inhibition efficiency and commercial availability, have been widely used; however, their effectiveness is limited to high concentrations and they can produce toxic vapors in acidizing environments [23, 24]. Synthetic chemists have been actively seeking environmentally friendly corrosion inhibitors that are free from heavy metals or toxic components, biodegradable and non-toxic themselves [25]. Research efforts have explored 'green' corrosion inhibitors, including plant extracts and commercial drugs that exhibit anti-corrosion properties [26–32]. Nevertheless, extracting corrosion inhibitors from natural products presents challenges, while the use of drugs as corrosion inhibitors is expensive and involves complex synthetic processes [33–40]. In recent years, significant attention has been given to five-membered heterocyclic compounds, specifically oxazoles, which have demonstrated excellent anti-corrosion efficiency for various alloys and metals, including mild steel [41–45]. Oxazole-based compounds possess several advantages, such as being eco-friendly, cost-effective, easily synthesizable and effective at low concentrations, making them a promising alternative to traditional organic corrosion inhibitors. In our study, we focus on evaluating the effectiveness of 3-(1,3-oxazol-5-yl)aniline (3-OYA) (Figure 1) as a cost-effective and efficient corrosion inhibitor for mild steel in a 1-M HCl solution. We investigate the inhibition efficiency at different concentrations, immersion periods and temperatures using weight loss measurements, potentiodynamic polarization (PDP) and electrochemical impedance spectroscopy (EIS) techniques. Additionally, we measure and/or calculate the thermodynamic parameters and analyze the molecular structure by conducting a geometry optimization of 3-OYA and utilizing density functional theory (DFT) to explore the relationship between inhibition activity and molecular structure.

2 CORROSION AND ITS EFFECTS ON SOCIETY AND THE ECONOMY

Corrosion is a naturally occurring process that gradually deteriorates the physical and chemical properties of metals and alloys when they react with their environment. Corrosion has significant social and economic impacts. In terms of social effects, corrosion can negatively affect human health and safety, as it weakens the structural integrity of metal structures, such as bridges, pipelines and buildings, increasing the risk of collapse or failure. It can also lead to the release of hazardous materials, such as lead into the environment, posing a threat to human health [46, 47]. Economically, corrosion can have a substantial impact on industries and infrastructure. The direct costs of corrosion include repairing or replacing damaged equipment, lost productivity due to downtime and increased maintenance and inspection costs. The global cost of corrosion was estimated to be $2.5 trillion in 2019, representing approximately 3.4% of global GDP. Corrosion can also have indirect economic impacts, such as reduced competitiveness of businesses, decreased property values and reduced tax revenues for governments. For instance, corrosion of water supply infrastructure can lead to reduced water quality, which can negatively impact tourism and local economies [47, 49]. To mitigate the negative effects of corrosion, implementing corrosion prevention and control measures is essential. These measures can include the use of corrosion-resistant materials, protective coatings and cathodic protection systems. By implementing these measures, the direct and indirect costs of corrosion can be reduced and human health and safety can be improved.

In conclusion, corrosion has significant social and economic impacts, including risks to human health and safety, direct costs associated with equipment repair and replacement and indirect costs, such as reduced competitiveness and decreased property values. Implementing effective corrosion prevention and control measures is crucial to mitigate these impacts.

3 COMPREHENSIVE ANALYSIS OF THE STRUCTURE–ACTIVITY RELATIONSHIP OF OXAZOLE DERIVATIVES

Oxazole derivatives have shown promise as corrosion inhibitors due to their unique structural features and chemical properties. The structure–activity relationship of these compounds plays a crucial role in determining their inhibitory efficacy. Here, we provide a more detailed analysis of this relationship, considering the following aspects:

1. heterocyclic ring: The presence of the oxazole ring in the molecular structure of oxazole derivatives contributes to their corrosion inhibition properties. The aromatic nature of the ring allows for effective π-electron interactions with the metal surface, leading to the formation of a protective film. Different modifications of the oxazole ring, such as substitution patterns and ring fusion, can influence the inhibitory efficacy by altering the electronic distribution and steric effects.
2. functional groups and substituents: The presence of functional groups and substituents in oxazole derivatives can significantly affect their inhibitory activity. Various groups, such as amino, hydroxyl, carboxyl and sulfonic acid groups, have been incorporated into the molecular structure to enhance the adsorption and interaction with the metal surface. Comparative studies have demonstrated that specific functional groups can improve the inhibitory efficiency by providing additional adsorption sites or enhancing the polarizability of the molecule.
3. molecular size and geometry: The size and geometry of oxazole derivatives also influence their inhibitory activity. The

molecular size affects the steric hindrance, which can impact the accessibility of the inhibitor to the metal surface. Additionally, the molecular geometry, including planarity and spatial arrangement of functional groups, can affect the strength and orientation of the inhibitor-metal interaction.

Comparative literature evidence supports the notion that the structure–activity relationship of oxazole derivatives in corrosion inhibition is complex and multifaceted. Studies have explored the impact of structural modifications on inhibitory performance, including variations in substituents, ring fusion and functional groups. These investigations have provided insights into the specific molecular interactions between the inhibitor and the metal surface, shedding light on the mechanism of inhibition.

In the case of 3-OYA, its inhibitory efficacy can be attributed to the presence of both the oxazole ring and the aniline moiety. The oxazole ring contributes to the formation of a protective adsorption layer on the mild-steel surface, while the aniline moiety provides additional sites for interaction with the metal surface. This combination of structural features enhances the inhibitory performance of 3-OYA and makes it an effective corrosion inhibitor for mild steel in 1 M HCl solution.

By considering the structure–activity relationship and drawing upon comparative literature evidence, we aim to provide a comprehensive analysis of how the structural features of oxazole derivatives, including 3-OYA, influence their corrosion inhibition properties. This analysis contributes to a deeper understanding of the molecular factors that govern the inhibitory efficacy, paving the way for the design and development of more effective corrosion inhibitors in the future.

4 EXPERIMENTAL

4.1 Weight loss measurements

The Metal Samples Company provided mild steel coupons for the study, each with a composition (wt. %) of carbon (0.210), manganese (0.050), silicon (0.380), aluminum (0.010), sulphur (0.050), phosphorus (0.090) and iron. To investigate their corrosion behavior, the coupons were subjected to weight loss measurements and electrochemical techniques. Prior to testing, the mild steel coupons were pre-treated by grinding with emery paper, washing with double-distilled water, degreasing with ethanol and drying at room temperature. To create a corrosive solution, 1 M hydrochloric acid was prepared by diluting 37% analytical-grade HCl (Merck-Malaysia) with double-distilled water, and varying amounts of 3-OYA were added to adjust the concentration. The coupons were then immersed in the solution for a specified period of time and evaluated for any signs of corrosion or degradation. Corrosion rate (C_R), inhibition efficiency (IE%) and surface coverage (θ) were calculated using weight loss measurements as per the NACE standard. The experiments were conducted at different 3-OYA concentrations, temperatures and immersion times to determine the efficacy of 3-OYA as a corrosion inhibitor in acidic media. The corrosion parameters were calculated using Equations (1)–(3) [52].

$$C_R = \frac{W}{at} \tag{1}$$

$$IE\% = \left[1 - \frac{C_{R(i)}}{C_{Ro}}\right] \times 100 \tag{2}$$

$$\theta = 1 - \frac{C_{R(i)}}{C_{Ro}} \tag{3}$$

4.2 Adsorption isotherms

Analyzing the adsorption isotherm type can provide valuable insights into the characteristics of the tested compounds. The surface coverage (θ) of inhibitors can be determined by applying different adsorption isotherms, such as Langmuir, Frum-kin and Temkin. In this study, the surface coverage (θ) values for various inhibitor concentrations in acidic media were determined using weight loss measurements. A scale with a sensitivity of 0.001 g was used for the weight loss measurements, and the samples had dimensions of 1.0 cm × 1.0 cm × 0.1 cm.

4.3 EIS and PDP measurements

The electrochemical assessment was conducted using a Potentiostat/Galvanostat/ZRA instrument and software developed by Gamry in a three-electrode setup with a reference electrode of a saturated calomel electrode and a metal working electrode with an exposed area of 4.5 cm2 that was cleaned in accordance with ASTM G1–03 [50]. The tests were conducted three times, and the inhibitive efficacy was evaluated using Equation (4).

$$IE\,(\%) = \frac{\mathrm{i_{corr}} - \mathrm{i_{corr(inh)}}}{\mathrm{i_{corr}}} \times 100 \tag{4}$$

The current density in the presence/absence of the tested inhibitor molecules was evaluated using Equation (4). The working electrode was cleaned according to ASTM G1–03 [51, 52] and had an exposed area of 4.5 cm2. Tafel curves were obtained by scanning from 0.25 V to +0.25 V SCE at a rate of 0.5 mVs1, 30 minutes after immersing the working electrode in the acidic solution at a constant temperature of 303 K. Electrochemical impedance tests (EIS) were carried out using a three-electrode setup, where the reference electrode was a saturated calomel electrode, and the working electrode was made of metal. The EIS results were analyzed using appropriate equivalent circuits and the Gamry Echem Analyst tool. Inhibitory activity (IE%) was calculated using Formula (5) based on the charge transfer impedance.

$$IE\,(\%) = \frac{R'_{ct} - R_{ct}}{R'_{ct}} \times 100 \tag{5}$$

where R'_{ct} is the charge transfer resistances in treated solution and R_{ct} is the charge transfer resistances in untreated solution.

4.4 DFT calculations

The quantum chemistry calculations were performed with Gaussian 09 software [53]. The inhibitor structure was optimized using the B3LYP method and a 6-31G++(d,p) basis set, in the gas phase. The ionization potential (I) and electron affinity (A) were calculated as E_HOMO and E_LUMO, respectively, based on Koopman's theorem [54, 55], using Equations (6) and (7).

$$I = -E_{HOMO} \tag{6}$$

$$A = -E_{LOMO} \tag{7}$$

The calculation of quantum chemical parameters, such as electronegativity (χ), hardness (η), softness (σ) and transferred electrons fractional number (ΔN) [56, 57] was performed using Equations (8)–(11):

$$\chi = \frac{I + A}{2} \tag{8}$$

$$\eta = \frac{I - A}{2} \tag{9}$$

$$\sigma = \eta^{-1} \tag{10}$$

$$\Delta N = \frac{7 - \chi_{inh}}{2\,(\eta_{inh})} \tag{11}$$

The electronegativity and hardness of the inhibitor can be represented by χ_{inh} and η_{inh}, respectively (with reference to Fe as χFe = 7 eV and ηFe = 0 eV), which are calculated as per Equations (8) and (9).

5 RESULTS AND DISCUSSION

5.1 Effects of inhibitor concentrations, immersion periods and temperatures

The study found that increasing the concentration of 3-OYA improved its anticorrosion performance. The highest inhibitory efficiency of 93.5% was achieved at a concentration of 0.5 mM 3-OYA due to the presence of amino group in the inhibitor structure that formed coordination bonds with the metal surface, resulting in a more efficient protective layer against corrosion [58–63]. The molecular structure and chemical composition of 3-OYA play a crucial role in its ability to prevent corrosion. Aromatic groups and functional groups, such as amino group, enhance the interactions of 3-OYA molecules with iron atoms on the metallic substrate, resulting in an effective corrosion inhibitor. Several studies have investigated the effect of different concentrations of corrosion inhibitors on mild steel corrosion rates in acidic solutions. While higher concentrations of inhibitors generally lead to lower corrosion rates, the optimal concentration may depend on the specific inhibitor and on other variables, such as temperature and the presence of other ions in the solution. Some inhibitors may become less effective at high concentrations or even become corrosive themselves [64–66]. For 3-OYA, increasing the concentration beyond 0.5 mM has little effect (Figure 2) on inhibitory efficiency since the protective film formed by the 3-OYA molecules acts as a barrier to corrosive agents and prevents the substrate from being attacked. Therefore, the molecular structure and chemical composition of inhibitors play a critical role in their effectiveness in preventing corrosion, and it is recommended to consult literature specific to the chosen inhibitor to determine the ideal concentration for corrosion inhibition. In conclusion, 3-OYA molecules have proven to be effective corrosion inhibitors in acidic environments, and increasing the concentration up to 0.5 mM can significantly reduce the corrosion rate and protect the metal surface by forming a stable and protective film [67–69].

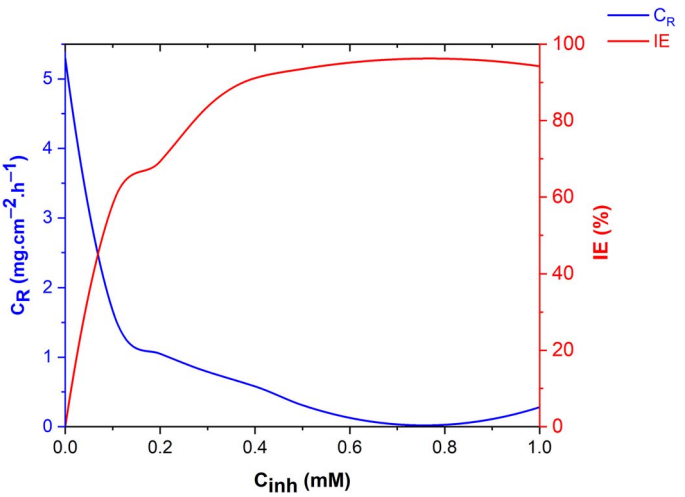

Figure 2. *CR and IE% of mild steel immersed in a corrosive environment for 5 h at 303 K for different concentrations of 3-OYA.*

To investigate the effectiveness of 3-OYA in reducing/preventing corrosion, mild steel samples were exposed to 1 M HCl supplemented with varying concentrations of 3-OYA (ranging from 0.1 to 1.0 mM) for immersion periods ranging from 1 to 48 hours at a temperature of 303 K. Figure 3 shows the effect of 3-OYA concentrations on the corrosion rate and inhibitory efficiency of metallic coupons at different immersion periods.

The results demonstrated (Figure 4) a significant reduction in the corrosion rate as the concentration of 3-OYA increased, with the highest inhibitory efficacy achieved at 1.0 mM 3-OYA concentration, resulting in a decrease of almost 70% compared to the 0.1-mM 3-OYA concentration. Additionally, the immersion time had a significant effect on the inhibitory efficiency of 3-OYA, with a longer immersion time resulting in a higher inhibitory effect. For instance, at 1.0 mM 3-OYA concentration, the corrosion rate was lowest after 48 hours of immersion, with an 80% decrease compared to the 1-hour immersion time. The inhibitory efficiency of 3-OYA on metal substrates increases rapidly with immersion duration up to 10 hours, remains constant from 10 to 24 hours and gradually decreases from 24 to 48 hours. The adsorption of 3-OYA molecules onto the metal substrate enhances the inhibitory effect due to the increased concentration of 3-OYA

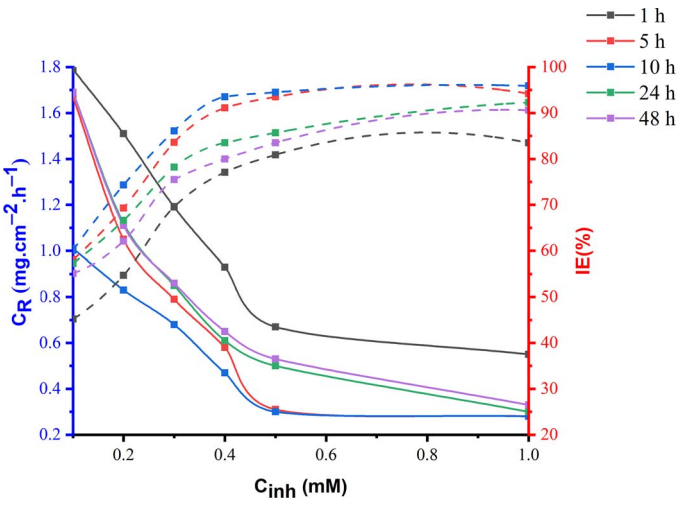

Figure 3. *CR and IE% of mild steel immersed in a corrosive environment for various exposure time at 303 K for different concentrations of 3-OYA.*

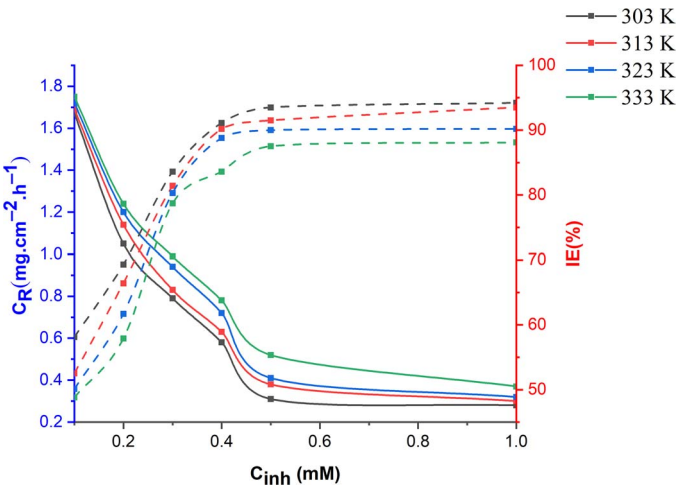

Figure 4. *3-OYA concentrations effect on the rate of corrosion and inhibitory efficiency of metallic coupons in 1 M HCl at different temperatures for 5 h.*

molecules, forming a uniform coating of 3-OYA that acts as a barrier to prevent corrosion. However, an immersion period exceeding 24 hours results in the depletion of 3-OYA molecules due to their reaction with the metal surface, leading to a gradual decrease in inhibitory efficacy. The inhibitory efficacy of 3-OYA is influenced by several factors, including temperature, pH and solution concentration, which should be carefully controlled for optimal inhibitory efficiency. The maximum inhibitory efficacy is achieved between 10 to 24 hours of immersion period due to strong hydrogen bonding and coordination interactions between the inhibitor molecules and the metal substrate. The high adsorption density of 3-OYA leads to physisorption and chemisorption, contributing to the stability and efficacy of 3-OYA as a corrosion inhibitor in acidic environments. Although the inhibitory activity of 3-OYA may decrease if some inhibitor molecules escape the surface, the 3-OYA layer's stability is high, resulting in a reasonably high inhibitory efficacy during prolonged exposure periods. This inhibits the access of corrosive agents to the metal surface, reduces the corrosion rate, and thus increases the inhibitory efficacy of 3-OYA. Overall, these findings suggest that 3-OYA could be a potential alternative to traditional corrosion inhibitors for protecting metal surfaces.

The study investigated the impact of temperature on the corrosion inhibition of metallic substrate by 3-OYA at different concentrations (0.1–1.0 mM) using mass reduction technique after 5 hours of immersion at temperatures ranging from 303 to 333 K. Results indicated that as temperature increased, the rate of corrosion increased and the corrosion efficiency of 3-OYA decreased. This could be due to the increase in the activity of corrosive species in the solution at higher temperatures, reducing the effectiveness of 3-OYA as a corrosion inhibitor. Additionally, the thermodynamic instability of 3-OYA at elevated temperatures could cause it to break down, making it less effective in inhibiting corrosion. The rate of reaction between 3-OYA and the metallic substrate may also increase with temperature, leading to the consumption of the inhibitor and further reduction in its inhibition efficiency [71].

At all concentration levels, 3-OYA exhibited a decrease in inhibitory potency with rising temperature, indicating physisorption. Additionally, inhibition efficiencies of 3-OYA were investigated at temperatures of 303, 313, 323 and 333 K, and results showed that 3-OYA exhibited significant inhibition efficiency at 0.5 mM, with considerable inhibitive performance. The inhibition efficiency of 3-OYA decreased slightly as temperature increased, especially at the highest tested inhibitor concentration (1 mM), which can be attributed to both chemical and physical adsorption mechanisms. The findings suggest that the inhibition efficiency of 3-OYA primarily depends on the temperature of the environment. These findings can be used to optimize the conditions under which 3-OYA can be used as a corrosion inhibitor for mild steel.

In our study, we observed that the inhibitor efficiency of 3-(1,3-oxazol-5-yl)aniline (3-OYA) decreases with increasing temperature. This is a common trend observed in many corrosion inhibition studies and can be attributed to several factors:

1. activation energy: corrosion reactions are typically thermally activated processes, meaning that higher temperatures provide additional energy for the corrosion reaction to occur. As the temperature increases, the activation energy barrier for the corrosion process decreases, resulting in a more rapid corrosion rate. In the presence of an inhibitor, the inhibitor molecules adsorb onto the metal surface and form a protective barrier, hindering the corrosion reaction. However, at higher temperatures, the thermal energy can disrupt the adsorption of inhibitor molecules, reducing their effectiveness in forming a protective layer.
2. adsorption process: the adsorption of inhibitors onto the metal surface is a crucial mechanism for corrosion inhibition. At lower temperatures, the adsorption of inhibitor molecules is typically more favorable due to lower thermal agitation and increased molecular interactions with the metal surface. This

facilitates the formation of a stable and compact inhibitor film on the metal surface, effectively reducing the corrosion rate. However, as the temperature increases, the thermal energy becomes more dominant, leading to weaker adsorption forces and reduced inhibitor coverage on the metal surface. Consequently, the protective film formed by the inhibitor becomes less effective in preventing corrosion.

3. molecular structure: The molecular structure of the inhibitor can also influence its performance at different temperatures. Some inhibitors may exhibit better stability and stronger adsorption at lower temperatures due to specific interactions with the metal surface or solvent molecules. However, at elevated temperatures, these interactions may weaken or change, affecting the inhibitor's ability to form an effective protective layer.

It is important to note that while the inhibitor efficiency decreases with increasing temperature, it does not imply that the inhibitor is completely ineffective at higher temperatures. Inhibitors can still provide some degree of corrosion protection, albeit at a reduced level, even under elevated temperature conditions. However, it is crucial to optimize the inhibitor concentration and application method to ensure adequate corrosion protection at higher temperatures.

In summary, the observed decrease in inhibitor efficiency with increasing temperature in our weight loss experiment is consistent with the general understanding of corrosion inhibition behavior. The increased thermal energy and its effect on the adsorption process, activation energy and molecular interactions contribute to the reduced performance of the inhibitor at higher temperatures. These findings emphasize the importance of considering temperature as a critical parameter when evaluating the applicability and effectiveness of corrosion inhibitors in practical applications.

5.2 Adsorption isotherm

The adsorption isotherm was used to understand how the particles of the inhibitor interact with the metallic substrate. To determine which isotherms matched the findings, surface coverage values were collected for the 3-OYA through gravimetric tests. The Temkin, Freundlich and Langmuir isotherms were used to investigate the adsorption mechanism. The Langmuir isotherm model best described the adsorption process, indicating that it was a monolayer process with a fixed maximum capacity. The Temkin isotherm model suggested that the adsorption process was controlled by the heat of adsorption, while the Freundlich isotherm model suggested that the adsorption process was controlled by the heterogeneity of the adsorbent surface and was a multi-layer process. The Langmuir isotherm model is useful for determining the maximum capacity of the adsorbent and metal ion uptake under different conditions, while the Temkin and Freundlich isotherms provide insight into the nature of the adsorption process and the role of heat and surface heterogeneity, respectively. These results can help in the design and optimization of adsorption processes for the removal of metal ions from aqueous solutions. The Langmuir adsorption isotherms matched the data well, according to the regression coefficient (R2) for 3-OYA of 0.99629. Table 1 represents the thermodynamic parameters.

Table 1. *Thermodynamic parameters of the tested compound in various Temperature*

Parameter	303 K	313 K	323 K	333 K
R2	0.172	0.190	0.1996	0.204
Slop	0.978 ± 0.029	0.970 ± 0.033	1.000 ± 0.047	1.018 ± 0.048
Intercept	0.067 ± 0.015	0.082 ± 0.016	0.085 ± 0.02	0.095 ± 0.024

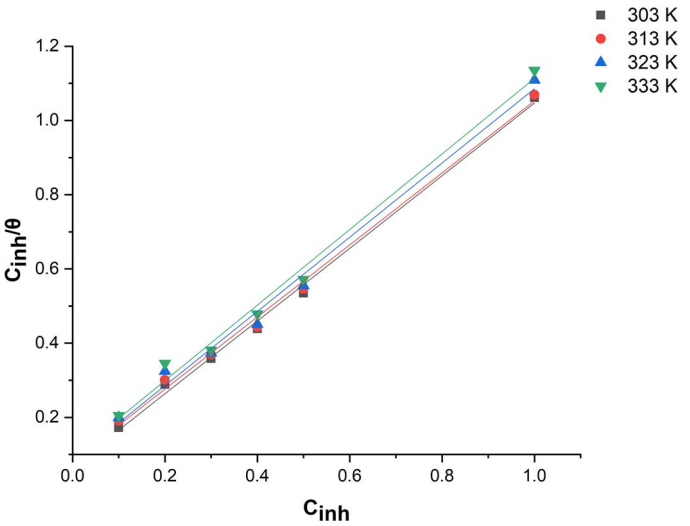

Figure 5. *The Langmuir isotherm for a mild steel in an acidic environment that has been inhibited by various inhibitor concentrations.*

Figure 5 shows the Langmuir adsorption isotherm plot between C_{inh}/θ and C_{inh}. The adsorption parameters can be determined using Equation (12).

$$C_{inh}/\theta = (K_{ads})^{-1} + C \tag{12}$$

The concentration of 3-OYA is denoted by C_{inh}, while θ represents the surface area, and K_{ads} is the equilibrium constant. The adsorption parameters, ΔG^{o}_{ads} and K_{ads}, were determined by evaluating the plot between C/θ and C. The adsorption parameters were calculated using Equation (13).

$$\Delta G^{o}_{ads} = -RT \ln (55.5 K_{ads}) \tag{13}$$

The expression includes the value 55.5 to represent the molar concentration of water, as well as the universal gas constant (R) and absolute temperature (T).

According to references [72, 73], the mechanism of adsorption can be determined by the ΔG^{o}_{ads} value, where a value of approximately -40 kJ•mol^{-1} suggests a chemisorption mechanism, while

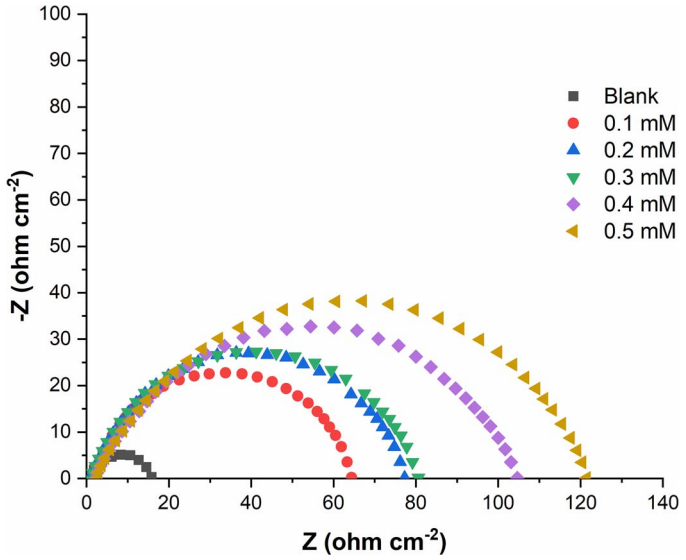

Figure 6. *The Nyquist plots of mild steel in untreated and treated hydrochloric acid solution.*

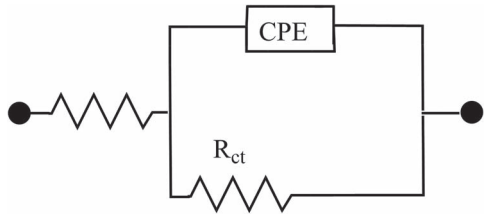

Figure 7. *The Randles circuit.*

Table 2. *EIS parameters for mild steel corrosion in uninhibited and inhibited 1 M corrosive solution at 303 K*

Conc. (mM)	R_{ct} (Ω cm^2)	C_{dl} (Ω cm^2)	IE (%)
0	11.9	284.9	-
0.1	78.4	87.7	70.4
0.2	89.7	71.9	76.3
0.3	103.2	64.2	81.2
0.4	117.8	53.6	85.3
0.5	137.9	38.7	90.6

a value of approximately −20 kJ•mol^{-1} indicates physisorption. In the case of 3-OYA, the ΔG^o_{ads} value was found to be of −32.17 kJ•mol^{-1}, indicating a combination of both chemisorption and physisorption mechanisms. This suggests that the adsorption process involves both chemical and physical interactions and is exothermic and spontaneous due to the negative value of ΔG^o_{ads}. The magnitude of the value suggests that the chemisorption mechanism dominates, resulting in a stable and irreversible adsorption of 3-OYA molecules through strong chemical bonds. However, the value's proximity to −20 kJ•mol^{-1} also implies some contribution from physical interaction, which is often observed in real-world systems with a combination of both chemical and physical interactions.

5.3 EIS and PDP measurements

Electrochemical impedance spectroscopy (EIS) has been widely used for quantifying and mitigating corrosion. Figure 6 shows the impedance spectra of mild steel corrosion in 1 M HCl at 303 K with and without 3-OYA, with concentration ranges of 0.1 to 0.5 mM, displayed in Nyquist plots. The Nyquist plots for both inhibited and uninhibited solutions show capacitive semi-circles, indicating charge transfer across the metal/solution interface during the corrosion process. The non-perfect semi-circular nature of Nyquist plots, with their centers below the real impedance axis, is due to unavoidable frequency dispersion caused by inhomogeneity and mass transfer on the solid surfaces [74]. The addition of inhibitor up to 0.5 mM concentrations increases the diameter of the semi-circle, which is associated with an increase in the charge transfer resistance (R_{ct}) at the metal/solution interface. Corrosion parameters, such as Rct, double layer capacitance (C_{dl}), phase shift (n) and corrosion rate (CR), can be extracted by fitting the response using equivalent circuits that describe the charge

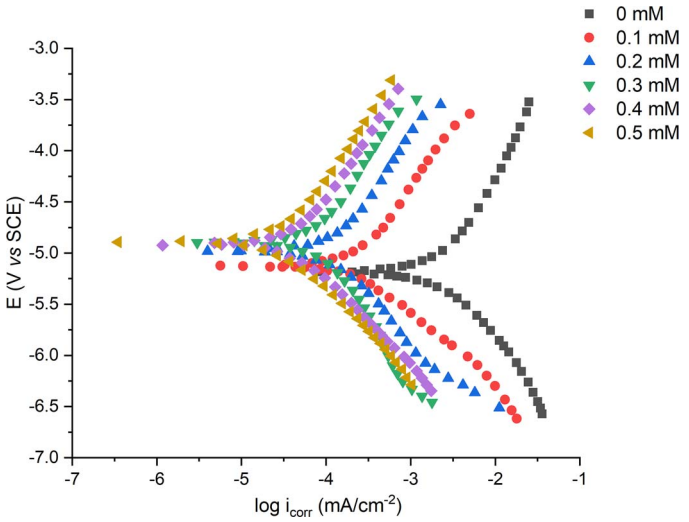

Figure 8. *The PDP plots of mild steel in untreated and treated hydrochloric acid solution.*

transfer kinetics of the electrode reactions. Percentage inhibition efficiency (IE) was derived from Rct using the following equation [75].

The Randles circuit, consisting of a solution resistance (R_s), double layer capacitance (C_{dl}) and charge transfer resistance (Rct), was determined to be the most appropriate equivalent circuit for electrode reactions involving double layer capacitance. To overcome the challenges associated with interpreting the depressed semi-circle, a constant phase element (CPE) was introduced into the Randles circuit instead of capacitance. Figure 7 shows the modified Randles circuit. The magnitude of the CPE can be calculated [76] using equation (14).

Table 3. *PDP parameters for mild steel corrosion in uninhibited and inhibited acidic solution at 303 K*

Conc. mM	$-E_{corr}\ (mV)$	$\beta_c\ (mVdec^{-1})$	$\beta_a\ (mVdec^{-1})$	$i_{corr}\ (Acm^{-1})$	IE(%)
Blank	486	101.12	120.93	1.672	-
0.1	498	87.69	102.18	0.077	76.2
0.2	509	83.28	96.48	0.041	8193
0.3	515	78.33	89.28	0.030	88.4
0.4	518	75.99	87.63	0.021	92.8
0.5	520	74.92	83.54	0.018	94.7

The Z_{CPE} can be calculated using equation (14) provided, where Y_0 represents admittance and measures the ease of current flow through the device, ω is the angular frequency, j is the imaginary number and n represents the phase shift between circuit elements due to surface changes.

$$Z_{CPE} = \left(\frac{1}{Y_0}\right)\left[(j\omega)_n\right]^{-1} \tag{14}$$

The double layer capacitance of the system, which includes the CPE, is given regarding to equation (15).

$$C_{dl} = \left(Y_0 R_{ct}^{1-n}\right)^{1/n} \tag{15}$$

Table 2 presents various impedance parameters obtained by non-linear square fitting of impedance data to the Randles circuit. The data in the table indicates an increase in Rct values with increasing 3-OYA concentration, with a maximum value observed at 0.5 mM and 303 K [77]. The introduction of an inhibitor significantly reduced the double layer capacitance, indicating the quasi-substitution of highly dielectric water molecules by a low dielectric organic inhibitor molecule. This resulted in an increase in the thickness of the double layer and a reduction in the number of active corrosion sites, as indicated by the Helmholtz Model equation (16).

$$C_{dl} = \frac{\epsilon_0 \epsilon_s A}{d} \tag{16}$$

The process of corrosion can be studied using potentiodynamic polarization (PDP), which allows for the investigation of the kinetics of the anodic and cathodic reactions. A study was conducted on the effect of 3-OYA on mild steel in 1 M HCl using polarization curves, as shown in Figure 8. The addition of 3-OYA resulted in a significant reduction in the corrosion rate, as evidenced by the shift of the cathodic and anodic curves to more negative and positive potentials, respectively. This shift may be due to the adsorption of the inhibitor on the metal surface. The corrosion potential (E_{corr}), corrosion current density (i_{corr}), anodic and cathodic Tafel slopes (β_a and β_c) were determined using Tafel extrapolation towards E_{corr}values.

The inhibition efficiency was calculated using Equation (4) and the results are presented in Table 3. As the dosage of the inhibitor increased, the corrosion rate and corrosion current density decreased, and the anodic and cathodic reactions were decelerated. The inhibitor exhibited mixed type behavior with a pro-cathodic tendency, as evidenced by the changes in both anodic and cathodic Tafel slopes. The polarization resistance (R_p) was determined using the Stern-Geary equation. The inhibitive effect of 3-OYA was remarkable, as demonstrated by the comparable inhibition efficiencies obtained from all the studied techniques [78–83].

$$R_p = \frac{\beta_a \beta_c}{2.303 \times i_{corr}\,(\beta_a + \beta_c)} \tag{17}$$

5.4 DFT

The reactivity of the inhibitor molecule and its interactions with the metal surface were studied using the frontier molecular orbital (FMO) theory and Mullikan charges. FMO theory suggests that the highest occupied molecular orbital (HOMO) and lowest unoccupied molecular orbital (LUMO) levels of the reacting species determine their chemical reactivity. Figure 9 shows the optimized geometry, HOMO and LUMO of the 3-OYA molecule, while Table 4 presents various quantum chemical parameters [84]. The HOMO density is primarily located over the aniline ring, and the LUMO is over the aniline and oxazole rings. A high EHOMO value indicates enhanced corrosion inhibition efficiency because it represents the species' capacity to donate electrons and form coordinate type bond with the empty d orbitals of metal atoms.

Conversely, a low ELUMO value suggests a favorable condition for accepting electrons by back donation from iron atoms. The 3-OYA molecule has a relatively high EHOMO and reasonably low ELUMO values, which enable it to donate electrons to metal atoms and accept electrons under favorable conditions, making it a good corrosion inhibitor. The energy gap (ΔE = ELUMO − EHOMO) is a measure of corrosion inhibition, and a lower ΔE signifies the lower kinetic stability of the molecule with more polarizable nature, making it easier to adsorb on the metal surface [85]. The Mullikan charges (Figure 10) were conducted to determine the inhibitor molecule's point of approach to the metal surface. The more negative the atomic charges, the more likely it is to donate electrons to the metal surface and preferentially get adsorbed via a donor-acceptor type interaction [84]. The nitrogen atom of the

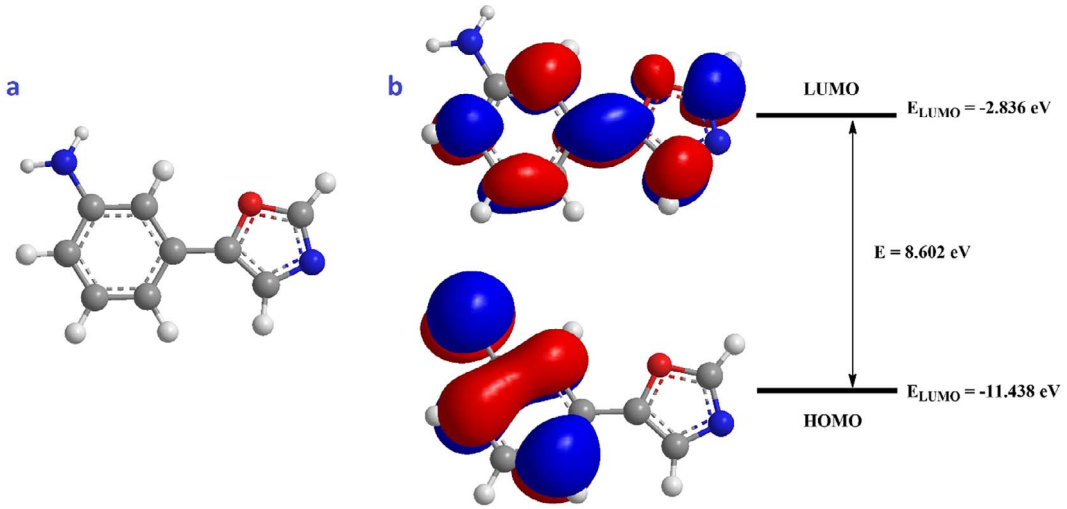

Figure 9. *(a) Optimized structure and (b) Band gap diagram of 3-OYA molecule*

Table 4. *Quantum chemical parameters of 3-OYA molecule*

I (eV)	A (eV)	E_{HOMO} (eV)	E_{LUMO} (eV)	ΔE (eV)	χ (eV)	η (eV)	σ (eV^{-1})	ΔN (eV)
11.43	2.836	-11.4338	-2.836	8.5978	7.1349	4.29	0.23	0.0157

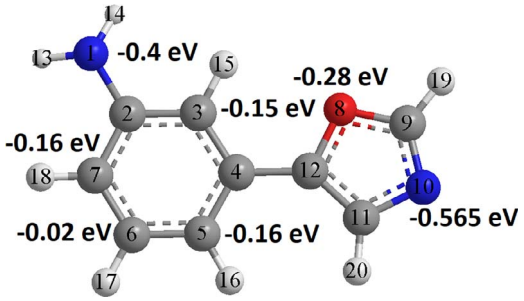

Figure 10. *Atomic charges of 3-OYA molecule*

aniline and oxazole rings (N1 and N10) and oxygen atom (O8) have the highest negative charge densities, indicating that they are the most apparent reactive centers for adsorption.

5.5 Suggestion inhibition mechanism

Corrosion inhibition in a solution is typically attributed to the adsorption of the inhibitor onto the metal surface, which is influenced by factors, such as the aggressive media type, metal nature and charge and inhibitor charge and dipole moment [86]. The adsorption mechanism is complex and not easy to predict due to the nature of corrosion and adsorption. Mild steel surface carries positive charges in acidic media both in the absence and presence of inhibitors, as shown by zero charge potential analysis [87]. Cl ions are suggested to adsorb first, creating excess negative charges toward the mild steel surface in acidic solution [88, 89]. The protonated form of the inhibitor may interact with the negatively charged metal/solution interface to form a protective film, preventing the metal from contacting the aggressive medium (physisorption), as proposed by some researchers [90, 91]. Alternatively, the inhibitor may form coordinate bonds with the d-orbital of Fe atoms and the lone pair of sp2 electrons of hetero atoms and pi electrons of the benzene ring (chemisorption). Therefore, both adsorption models may explain the effective corrosion inhibition properties of 3-OYA.

5.6 Comparison study

To the best of our knowledge, there have been no reports of corrosion inhibitors suitable for HCl solutions. The inhibition efficiency of 0.5 mM 3-OYA was found to be 93.5% at 303 K in a 1-M HCl solution, performing better than previously published inhibitors (Table 5), such as 2, 6, 8 to 12, 15 to 18, 20, 25, 26, 30 and 31. In the oil and gas industry, the bottom of the well is subjected to high temperatures, so a corrosion inhibitor must maintain its protective performance in corrosive media under such high temperatures.

In conclusion, the study showed that 3-OYA has the potential to be a highly effective corrosion inhibitor for mild steel protection in industrial applications. Its high inhibitory efficiency, adaptability and low toxicity make it a promising alternative to current inhibitors. Further studies should be conducted to evaluate the long-term performance and practical application of 3-OYA P in various industrial settings.

Table 5. *Comparison of 3-OYA with other nitrogen-based corrosion inhibitors for protecting mild steel*

No.	Inhibitor name	Alloy	Acid	IE(%)	Ref.
1.	3-OYA	Mild steel	1 M HCl	93.5	-
2.	N′-(2-(2-oxomethylpyrrol-1-yl)ethyl)piperidine	Mild steel	1 M HCl	91.9	[92]
3.	2-Amino-4-phenyl-N-benzylidene-5-(1,2,4-triazol-1-yl)thiazole	Mild steel	1 M HCl	98.1	[7]
4.	2-amino-4-phenylthiazole	Mild steel	1 M HCl	94.7	[9]
5.	1-Amino-2-mercapto-5-(4-(pyrrol-1-yl)phenyl)-1,3,4-triazole	Mild steel	1 M HCl	96.3	[93]
6.	N′-(2-hydroxybenzylidene)-2-(quinolin-8-yloxy)acetohydrazide	Mild steel	1 M HCl	93.4	[4]
7.	3-(4-ethyl-5-mercapto-1,2,4-triazol-3-yl)-1- phenylpropanone	Mild steel	1 M HCl	97	[10]
8.	4-ethyl-1-(4-oxo-4-phenylbutanoyl)thiosemicarbazide	Mild steel	1 M HCl	88.7	[2]
9.	4-benzyl-1-(4-oxo-4-phenylbutanoyl)thiosemicarbazide	Mild steel	1 M HCl	92.5	[11]
10.	4-chloro-2-((pyridin-2-ylimino)methyl)phenol	Mild steel	1 M HCl	92.8	[12]
11.	2-N-phenylamino-5-(3-phenyl-3-oxo-1-propyl)-1,3,4-oxadiazole	Mild steel	1 M HCl	95.1	[13]
12.	4-ethyl-1-(4-oxo-4-phenylbutanoyl)thiosemicarbazide	Mild steel	1 M HCl	88.7	[14]
13.	nonanedihydrazide	Mild steel	1 M HCl	97	[16]
14.	4-pyrrol-1-yl-n-(2,5-dimethyl-pyrrol-1-yl)benzoylamine	Mild steel	1 M HCl	95.8	[17]
15.	N´-(1-phenylethylidene)-4-(1H-pyrrol-1-yl)benzohydrazide	Mild steel	1 M HCl	94.5	[17]
16.	5-((4-fluorobenzylidene)amino)-1,3,4- thiadiazole-2-thiol	Mild steel	1 M HCl	91	[18]
17.	2-(5-amino-1,3,4-thiadiazol-2-yl)-5-nitrofuran	Mild steel	1 M HCl	83.2	[19]
18.	terephthalo- hydrazide	Mild steel	1 M HCl	96.4	[20]
19.	isophthalohydrazide	Mild steel	1 M HCl	97.2	[20]
20.	N-(Naphthalen-1yl)-1-(4-pyridinyl)methanimine	Mild steel	1 M HCl	91.5	[21]
21.	2-acetylthiophene thiosemicarbazon	Mild steel	1 M HCl	96	[22]
22.	2-isonicotinoyl-N-phenylhydrazinecarbothioamide	Mild steel	1 M HCl	96.3	[94]
23.	2-amino-5-(naphthalen-2-ylmethyl)-1,3,4-thiadiazole	Mild steel	1 M HCl	95.1	[46]
24.	5-(4-(1H-pyrrol-yl)phenyl)-2-mercapto-1,3,4-oxadiazole	Mild steel	1 M HCl	95	[41]
25.	N-(2,4-dihydroxytolueneylidene)-4-methylpyridin-2-amine	Mild steel	1 M HCl	93.7	[47]
26.	N-methyl-2-1-5-methylthiophene-2-yl)ethylidene) hydrazine carbothioamide	Mild steel	1 M HCl	95.3	[61]
27.	1-phenyl-2-(1-phenylethylidene)hydrazine	Mild steel	1 M HCl	83.8	[95]
28.	1-(1-(4-methoxyphenyl)ethylidene)-2-phenylhydrazine	Mild steel	1 M HCl	95.1	[96]
29.	2-(2,4-dimethoxybenzylidene)-Nphenylhydrazinecarbothioamide	Mild steel	1 M HCl	94.8	[97]
30.	2-(5-amino-1,3,4-oxadiazol-2-yl)-5-nitrofuran	Mild steel	1 M HCl	79.4	[98]
31.	8-piperazine-1-ylmethylumbelliferone	Mild steel	1 M HCl	93.4	[70]
32.	2-((6-methyl-2-ketoquinoUne-3-yl)methylene) hydrazinecarbothioamide	Mild steel	1 M HCl	95.8	[99]
33.	4-(6-methylcoumarin)acetohydrazide	Mild steel	1 M HCl	94.5	[52]
34.	4-(Benzoimidazole-2-yl)pyridine	Mild steel	1 M HCl	93.8	[48]
35.	5,5′-(1,4-phenylene)bis(N-phenyl-1,3,4-thiadiazol-2-amine)	Mild steel	1 M HCl	94	[49]
36.	APT	Mild steel	1 M HCl	95	[100]
37.	APT-2	Mild steel	1 M HCl	96	[100]
38.	APT-4	Mild steel	1 M HCl	92	[100]
39.	PAT	Mild steel	1 M HCl	98	[100]
40.	N (−benzo[d]thiazol-2-yl)-1-(thiophene-2-yl) methanimine (BTTM)	Mild Steel	H_2SO_4		[101]
41.	PMTTA	Mild steel	1 M HCl	92	[102]
42.	PATT	Mild steel	1 M HCl	91	[102]
43.	PMTA	Mild steel	1 M HCl	87	[102]

6 CONCLUSION

In conclusion, this study investigated the potential of 3-OYA as a corrosion inhibitor for mild steel in a hydrochloric acid solution. The results showed that 3-OYA exhibited excellent corrosion inhibition properties with a protection efficiency of 93.5% at a concentration of 0.05 mM. The inhibition efficiency increased with increasing inhibitor concentration but decreased with increasing temperature. The Langmuir adsorption isotherm was used to analyze the adsorption mechanism, revealing the formation of a protective adsorption layer on the mild-steel surface that inhibited the corrosion rate. Density functional theory (DFT) was employed to understand the correlation between the inhibition activity and the molecular structure, indicating that 3-OYA had high adsorption–inhibition activity. Overall, the results from both the experimental and theoretical analyses were consistent, suggesting that 3-OYA could be a promising candidate for use as a corrosion inhibitor for mild steel in acidic conditions. This study provides important insights into the fundamental mechanisms underlying the inhibitory process and paves the way for further research in this field.

DATA AVAILABILITY

All data will be available when request from the authors.

AUTHOR CONTRIBUTIONS

Ahmed Al-Amiery (Methodology-Equal, Supervision-Equal, Writing—original draft-Equal), Waleed K. Al-Azzawi (Investigation-Equal, Software-Equal).

ACKNOWLEDGEMENTS

The authors gratefully acknowledge the Universiti Kebangsaan Malaysia and University of Technology/Iraq for providing the facilities for this work.

REFERENCES

[1] Liu Y, Lv P, Gao L *et al.* A review on application of X-ray photoelectron spectroscopy in corrosion inhibition. *J Mater Sci Technol* 2019;**35**:717–26.
[2] Alamiery AA, Wan Isahak WNR, Takriff MS. Inhibition of mild steel corrosion by 4-benzyl-1-(4-oxo-4-phenylbutanoyl) thiosemicarbazide: gravimetrical, adsorption and theoretical studies. *Lubricants* 2021;**9**:93. https://doi.org/10.3390/lubricants9090093.
[3] Goudarziafshar H, Moradi L, Vafaei M, Asghari M. Corrosion inhibition of mild steel in acidic media using a new Schiff Base derivative: experimental and theoretical studies. *J Mol Liq* 2020;**303**:112693.
[4] Alkadir Aziz IA, Annon IA, Abdulkareem MH *et al.* Insights into corrosion inhibition behavior of a 5-mercapto-1,2,4-triazole derivative for mild steel in hydrochloric acid solution: experimental and DFT studies. *Lubricants* 2021;**9**:122. https://doi.org/10.3390/lubricants9120122.
[5] Al-Azzawi WK, Hussein SS, Salih SM *et al.* Efficient protection of mild steel corrosion in hydrochloric acid using 3-(5-Amino-1, 3, 4-thiadiazole-2yl)-2H-chromen-2-one, a Coumarin derivative bearing a 1, 3, 4-thiadiazole moiety: gravimetrical techniques, computational and thermodynamic investigations. *Prog. Color Colorants Coat.* 2023;**16**:97–111.
[6] Singh AK, Thakur S, Pani B *et al.* 2-Hydroxy-N-((thiophene-2-yl) methylene) benzohydrazide: ultrasound-assisted synthesis and corrosion inhibition study. *ACS Omega* 2018;**3**:4695–705.
[7] Alamiery A, Mohamad AB, Kadhum AAH, Takriff MS. Comparative data on corrosion protection of mild steel in HCl using two new thiazoles. *Data Brief* 2022;**40**:107838. https://doi.org/10.1016/j.dib.2022.107838.
[8] Ali N, Yusof MS, Khairul WM *et al.* The effect of concentration of *Lawsonia inermis* as a corrosion inhibitor for aluminum alloy in seawater. *Adv Phys Chem* 2017;**2017**:1–12. https://doi.org/10.1155/2017/8521623.
[9] Mustafa AM, Sayyid FF, Betti N *et al.* Inhibition of mild steel corrosion in hydrochloric acid environment by 1-amino-2-mercapto-5-(4-(pyrrol-1-yl)phenyl)-1,3,4-triazole. *S Afr J Chem Eng* 2022;**39**:42–51.
[10] Alamiery A. Short report of mild steel corrosion in 0.5 M H2SO4 by 4-ethyl-1-(4-oxo-4-phenylbutanoyl)thiosemicarbazide. *J Tribol* 2021;**30**:90–9.
[11] Dawood MA, Alasady ZMK, Abdulazeez MS *et al.* The corrosion inhibition effect of a pyridine derivative for low carbon steel in 1 M HCl medium: complemented with antibacterial studies. *Int. J. Corros. Scale Inhib.* 2021;**10**:1766–82.
[12] Alamiery A. Corrosion inhibition effect of 2-N-Phenylamino-5-(3-Phenyl-3-oxo-1-propyl)-1,3,4-oxadiazole on mild steel in 1 M hydrochloric acid medium: insight from gravimetric and DFT investigations. *Mater Sci Energy Technol* 2021;**4**:398–406.
[13] Alamiery AA. Anticorrosion effect of thiosemicarbazide derivative on mild steel in 1 M hydrochloric acid and 0.5 M sulfuric acid: gravimetrical and theoretical studies. *Mater Sci Energy Technol* 2021;**4**:263–73.
[14] Alamiery AA, Isahak WNRW, Aljibori HSS *et al.* Effect of the structure, immersion time and temperature on the corrosion inhibition of 4-pyrrol-1-yl-N-(2,5-dimethyl-pyrrol-1-yl)benzoylamine in 1.0 M HCl solution. *Int. J. Corros. Scale Inhib.* 2021;**10**:700–13.
[15] Zhang K, Xu B, Yang W *et al.* Halogen-substituted imidazoline derivatives as corrosion inhibitors for mild steel in hydrochloric acid solution. *Corros Sci* 2015;**90**:284–95.
[16] Al-Amiery AA, Mohamad AB, Kadhum AAH *et al.* Experimental and theoretical study on the corrosion inhibition of mild steel by nonanedioic acid derivative in hydrochloric acid solution. *Sci Rep* 2022;**12**:4705. https://doi.org/10.1038/s41598-022-08146-8.
[17] Alamiery A, Mahmoudi E, Allami T. Corrosion inhibition of low-carbon steel in hydrochloric acid environment using a Schiff Base derived from pyrrole: gravimetric and computational studies. *Int. J. Corros. Scale Inhib.* 2021;**10**:749–65.
[18] Eltmimi AJM, Alamiery A, Allami AJ *et al.* Inhibitive effects of a novel efficient Schiff Base on mild steel in hydrochloric acid environment. *Int. J. Corros. Scale Inhib.* 2021;**10**:634–48.
[19] Alamiery A, Shaker LM, Allami T *et al.* A study of acidic corrosion behavior of furan-derived Schiff Base for mild steel in hydrochloric acid environment: experimental, and surface investigation. *Mater Today Proc* 2021;**44**:2337–41.
[20] Al-Baghdadi SB, Al-Amiery AA, Gaaz TS, Kadhum AAH. Terephthalohydrazide and Isophthalo-hydrazide as new corrosion inhibitors for mild steel in hydrochloric acid: experimental and theoretical approaches. *Koroze Ochr Mater* 2021;**65**:12–22.
[21] Hanoon MM, Resen AM, Shaker LM *et al.* Corrosion investigation of mild steel in aqueous hydrochloric acid environment using n-(naphthalen-1yl)-1-(4-pyridinyl)methanimine complemented with antibacterial studies. *Biointerface Res Appl Chem* 2021;**11**:9735–43.
[22] Al-Baghdadi S, Gaaz TS, Al-Adili A *et al.* Experimental studies on corrosion inhibition performance of acetylthiophene thiosemicarbazone for mild steel in HCl complemented with DFT investigation. *Int J Low-Carbon Technol* 2021;**16**:181–8.
[23] Stupnišek-Lisac E, Podbršček S, Sorić T. Non-toxic organic zinc corrosion inhibitors in hydrochloric acid. *J Appl Electrochem* 1994;**24**:779–84.
[24] Quraishi A, Sardar R. Corrosion inhibition of mild steel in acid solutions by some aromatic oxadiazoles. *Mater Chem Phys* 2003;**78**:425–31.
[25] Quraishi MA, Jamal D. Corrosion inhibition of N-80 steel and mild steel in 15% boiling hydrochloric acid by a triazole compound-SAHMT. *Mater Chem Phys* 2001;**68**:283–7.
[26] Sinko J. Challenges of chromate inhibitor pigments replacement in organic coating. *Prog Org Coat* 2001;**42**:267–82.
[27] Hasson D, Shemer H, Sher A. State of the art of friendly "green" scale control inhibitors: a review article. *Ind Eng Chem Res* 2011;**50**:7601–7.
[28] Ji G, Shukla SK, Dwivedi P *et al.* Inhibitory effect of *Argemone mexicana* plant extract on acid corrosion of mild steel. *Ind Eng Chem Res* 2011;**50**:11954–9.
[29] Lebrini M, Robert F, Lecante A, Roos C. Inhibitory effect of *Argemone mexicana* plant extract on acid corrosion of mild steel. *Corros Sci* 2011;**52**:687–95.
[30] Deng Q, Ding NN, Wei XL *et al.* Identification of diverse 1,2,3-triazole-connected benzyl glycoside-serine/threonine conjugates as potent corrosion inhibitors for mild steel in HCl. *Corros Sci* 2012;**64**:64–73.
[31] Gece G. Drugs: a review of promising novel corrosion inhibitors. *Corros Sci* 2011;**53**:3873–98.
[32] Farsak M, Ongun YA, Kardaş G. Anticorrosion effect of 4-amino-5-(4-pyridyl)-4H-1,2,4-triazole-3-thiol for mild steel in HCl solution. *Chem Select* 2017;**2**:3676–82.
[33] Ashassi-Sorkhabi H, Majidi MR, Seyyedi K. Investigation of inhibition effect of some amino acids against steel corrosion in HCl solution. *Appl Surf Sci* 2004;**225**:176–85.
[34] Olivares-Xometl O, Likhanova NV, Domínguez-Aguilar MA *et al.* Synthesis and corrosion inhibition of α-amino acids alkylamides for mild steel in acidic environment. *Mater Chem Phys* 2008;**110**:344–51.

[35] Ghareba S, Omanovic S. Interaction of 12-aminododecanoic acid with a carbon steel surface: towards the development of 'green' corrosion inhibitors. *Corros Sci* 2010;**52**:2104–13. https://doi.org/10.1016/j.corsci.2010.02.019.

[36] Amin MA, Ibrahim MM. H2SO4 solutions by a newly synthesized glycine derivative. *Corros Sci* 2011;**53**:873–85.

[37] Hamani H, Douadi T, Daoud D *et al.* 1-(4-Nitrophenylo-imino)-1-(phenylhydrazono)-propan-2-one as a corrosion inhibitor for mild steel in 1m HCl solution: weight loss, electrochemical, thermodynamic and quantum chemical studies. *J Electroanal Chem* 2017;**801**:425–38.

[38] Prasai D, Tuberquia JC, Harl RR *et al. J Graphene: corrosion-inhibiting coating ACS Nano* 2012;**6**:1102–8.

[39] Kirkland NT, Schiller T, Medhekar N, Birbilis N. Exploring graphene as a corrosion protection barrier. *Corros Sci* 2012;**56**:1–4.

[40] Novoselov KS, Geim AK, Morozov SV *et al.* Electric field effect in atomically thin carbon films. *Science* 2004;**306**:666–9.

[41] Mustafa AM, Sayyid FF, Betti N *et al.* Inhibition evaluation of 5-(4-(1H-pyrrol-1-yl)phenyl)-2-mercapto-1,3,4-oxadiazole for the corrosion of mild steel in an acidic environment: thermodynamic and DFT aspects. *Tribologia* 2021;**38**:39–47.

[42] Fouda AS, Elmorsi MA, Fayed T, Said IAE. Oxazole derivatives as corrosion inhibitors for 316L stainless steel in sulfamic acid solutions. *Desalin Water Treat* 2016;**57**:4371–85.

[43] Rahmani H, El-Hajjaji F, Hallaoui AE *et al.* Experimental, quantum chemical studies of oxazole derivatives as corrosion inhibitors on mild steel in molar hydrochloric acid medium. *Int J Corros Scale Inhib* 2018;**7**:509–27.

[44] Dominguez-Crespo MA, ZepedaVallejo LG, Torres-Huerta AM *et al.* New triazole and isoxazole compounds as corrosion inhibitors for cu-Ni (90/10) alloy and galvanized steel substrates. *Metall Mat Trans A: Phys Metalld Mat Sci* 2020;**51**:1822–45.

[45] Ouzidan Y *et al.* Investigation of corrosion inhibition of mild steel in 1 M HCl by 3-methyl-4-(3-methyl-isoxazol5-yl)isoxazol-5(2H)-one monohydrate using experimental and theoretical approaches. *Der Pharma Chemica* 2016;**8**:294–303.

[46] Abdulazeez MS, Abdullahe ZS, Dawood MA *et al.* Corrosion inhibition of low carbon steel in HCl medium using a Thiadiazole derivative: weight loss, DFT studies and antibacterial studies. *Int. J. Corros. Scale Inhib.* 2021;**10**:1812–28.

[47] Abdulsahib YM, Eltmimi AJM, Alhabeeb SA *et al.* Experimental and theoretical investigations on the inhibition efficiency of N-(2,4-dihydroxytolueneylidene)-4-methylpyridin-2-amine for the corrosion of mild steel in hydrochloric acid. *Int. J. Corros. Scale Inhib.* 2021;**10**:885–99.

[48] Salman AZ, Jawad QA, Ridah KS *et al.* Selected BIS-thiadiazole: synthesis and corrosion inhibition studies on mild steel in HCL environment. *Surf Rev Lett* 2020;**27**:2050014.

[49] United States Environmental Protection Agency. The economic impact of corrosion. Available online: https://www.epa.gov/sites/production/files/2015-09/documents/corrosion.pdf (accessed on 1 March 2023).

[50] ASTM G 31-72. *Standard Guide for Laboratory Immersion Corrosion Testing of Metals*. Philadelphia, PA, USA: American Society for Testing and Materials, 1990.

[51] TM0169/G31-12a. *Standard Guide for Laboratory Immersion Corrosion Testing of Metals*. Houston, TX, USA: NACE International, 2012.

[52] Resen AM, Hanoon M, Salim RD *et al.* Gravimetrical, theoretical, and surface morphological investigations of corrosion inhibition effect of 4-(benzoimidazole-2-yl) pyridine on mild steel in hydrochloric acid. *Koroze Ochr Mater* 2020;**64**:122–30.

[53] Alamiery AA. Case study in a conceptual DFT investigation of new corrosion inhibitor. *Letters in Applied NanoBioScience* 2021;**11**:4007–15.

[54] McCafferty E. Validation of corrosion rates measured by Tafel extrapolation method. *Corros Sci* 2005;**47**:3202–15.

[55] Frisch, M.J.; Trucks, G.W.; Schlegel, H.B.; Scuseria, G.E.; Robb, M.A.; Cheeseman, J.R.; Scalmani, G.; Barone, V.; Mennucci, B.; Petersson, G.A.; *et al.* Gaussian; Gaussian, Inc.: Wallingford, UK, 2013.

[56] Koopmans T. Ordering of wave functions and eigenenergy's to the individual electrons of an atom. *Physica* 1934;**1**:104–13.

[57] Meyer YA, Menezes I, Bonatti RS *et al.* EIS investigation of the corrosion behavior of steel bars embedded into modified concretes with eggshell contents. *Metals* 2022;**12**:417. https://doi.org/10.3390/met12030417.

[58] Aljibori HS, Abdulzahra OH, Al Adily AJ *et al.* Corrosion inhibition effects of concentration of 2-oxo-3-hydrazonoindoline in acidic solution, exposure period, and temperature. *Int J Corros Scale Inhib* 2023;**12**:438–57.

[59] Al-Amiery AA, Rubaye AYI, Kadhum AAH, Al-Azzawi WK. Thiosemicarbazide and its derivatives as promising corrosion inhibitors: a mini-review. *Int J Corros Scale Inhib* 2023;**12**:597–620.

[60] Al-Amiery A, Isahak WNRW, Al-Azzawi WK. ODHI: a promising Isatin-based corrosion inhibitor for mild steel in hydrochloric acid. *J Mol Struct* 2023;**1288**:135829. https://doi.org/10.1016/j.molstruc.2023.135829.

[61] Khudhair AK, Mustafa AM, Hanoon MM *et al.* Experimental and theoretical investigation on the corrosion inhibitor potential of N-MEH for mild steel in HCl. *Prog Color Colorants Coat* 2021;**15**:111–22.

[62] Alamiery AA. Effect of temperature on the corrosion inhibition of 4ethyl-1-(4-oxo-4-phenylbutanoyl)thiosemicarbazide on mild steel in HCl solution. *Lett Appl NanoBioSci* 2021;**11**:3502–8.

[63] Betti N, Al-Amiery AA, Al-Azzawi WK, Isahak WNRW. Corrosion inhibition properties of Schiff base derivative against mild steel in HCl environment complemented with DFT investigations. *Sci Rep* 2023;**13**:8979.

[64] Obot IB, Haruna K, Saleh TA. Atomistic simulation: a unique and powerful computational tool for corrosion inhibition research. *Arabian J Sci Eng* 2019;**44**:1–32. https://doi.org/10.1007/s13369-018-3605-4.

[65] Lgaz H, Chung I-M, Salghi R *et al.* On the understanding of the adsorption of fenugreek gum on mild steel in an acidic medium: insights from experimental and computational studies. *Appl Surf Sci* 2019;**463**:647–58.

[66] Verma C, Lgaz H, Verma D *et al.* Molecular dynamics and Monte Carlo simulations as powerful tools for study of interfacial adsorption behavior of corrosion inhibitors in aqueous phase: a review. *J Mol Liq* 2018;**260**:99–120.

[67] Fang X, Zhang Y, Zhu L *et al.* Evaluation of organic corrosion inhibitors in HCl solution for mild steel protection. *Materials* 2020;**13**:3176.

[68] Mousa H, Al-Mobarak N. Effect of pomegranate peel extract on mild steel corrosion in HCl solution: experimental and theoretical studies. *Materials* 2020;**13**:2573.

[69] Olasunkanmi LO, Fayomi OSI, Abdulwahab M. Influence of castor oil concentration on the corrosion inhibition of mild steel in 1 M HCl solution. *Materials* 2018;**11**:1101.

[70] Hanoon MM, Resen AM, Al-Amiery AA *et al.* Theoretical and experimental studies on the corrosion inhibition potentials of 2-((6-methyl-2-ketoquinolin-3-yl)methylene) hydrazinecarbothioamide for mild steel in 1 M HCl. *Prog Color Colorants Coat* 2021;**15**:21–33.

[71] Betti N, Al-Amiery AA, Al-Azzawi WK. Experimental and quantum chemical investigations on the anticorrosion efficiency of a nicotinehydrazide derivative for mild steel in HCl. *Molecules* 2022;**27**:6254.

[72] Mahdi BS, Abbass MK, Mohsin MK *et al.* Corrosion inhibition of mild steel in hydrochloric acid environment using terephthaldehyde based on Schiff base: gravimetric, thermodynamic, and computational studies. *Molecules* 2022;**27**:4857. https://doi.org/10.3390/molecules27154857.

[73] Aziz IAA, Abdulkareem MH, Annon IA *et al.* Weight loss, thermodynamics, SEM, and electrochemical studies on N-2-methylbenzylidene-4-antipyrineamine as an inhibitor for mild steel corrosion in hydrochloric acid. *Lubricants* 2022;**10**:23. https://doi.org/10.3390/lubricants10020023.

[74] Karthik G, Sundaravadivelu M. Studies on the inhibition of mild steel corrosion in hydrochloric acid solution by atenolol drug, Egypt. *J Petrol* 2016;**25**:183–91.

[75] Mobin M, Aslam R, Aslam J. Non toxic biodegradable cationic gemini surfactants as novel corrosion inhibitor for mild steel in hydrochloric acid medium and synergistic effect of sodium salicylate: experimental and theoretical approach. *Mater Chem Phys* 2017;**191**: 151–67.
[76] Elemike EE, Onwudiwe DC, Nwankwo HU, Hosten EC. Synthesis, crystal structure, electrochemical and anti-corrosion studies of Schiff base derived from o-toluidine and o-chlorobenzaldehyde. *J Mol Str* 2017;**1136**:253–62.
[77] Verma C, Olasunkanmi LO, Obot IB *et al.* 2, 4-diamino-5-(phenylthio)-5 H-chromeno[2, 3-b] pyridine-3-carbonitriles as green and effective corrosion inhibitors: gravimetric, electrochemical, surface morphology and theoretical studies. *RSC Adv* 2016;**6**:53933–48.
[78] Hassan HH, Abdelghani E, Amin MA. Inhibition of mild steel corrosion in hydrochloric acid solution by triazole derivatives: part I. Polarization and EIS studies. *Electrochim Acta* 2007;**52**:6359–66.
[79] Abd El-Lateef HM, Tantawy AH. Synthesis and evaluation of novel series of Schiff base cationic surfactants as corrosion inhibitors for carbon steel in acidic/chloride media: experimental and theoretical investigations. *RSC Adv* 2016;**6**:8681–700.
[80] Ramya K, Mohan R, Joseph A *et al.* Interaction of benzimidazoles and benzotriazole: its corrosion protection properties on mild steel in hydrochloric acid. *JMEPEG* 2014;**23**:4089–101.
[81] Saranya J, Sounthari P, Parameswari K, Chitra S. Acenaphtho [1, 2-b] quinoxaline and acenaphtho [1, 2-b] pyrazine as corrosion inhibitors for mild steel in acid medium. *Measurement* 2016;**77**:175–86.
[82] Bahgat Radwan A, Sliem MH, Okonkwo PC *et al.* Corrosion inhibition of API X120 steel in a highly aggressive medium using stearamidopropyl dimethylamine. *J Mol Liq* 2017;**236**:220–31.
[83] Ahamad I, Prasad R, Quraishi MA. Adsorption and inhibitive properties of some new Mannich bases of Isatin derivatives on corrosion of mild steel in acidic media. *Corros Sci* 2010;**52**:1472–81.
[84] Kumar P, Dahiya S, Kumar R *et al.* An exhaustive study of a coupling reagent (1-(3- dimethylaminopropyl) 3-ethylcarbodiimide hydrochloride) as corrosion inhibitor for steel. *Ind J Chem Tech* 2017;**24**: 327–35.
[85] Fouda AS, Rashwan SM, Shaban SM *et al.* Evaluation of a novel cationic surfactant based on 2-(2 (dimethylamino)ethoxy)ethanol as a corrosion inhibitor for carbon steel 1018 in 1.0 M HCl solution. *Egypt J Petrol* 2018;**27**:295–306.
[86] Ma H, Chen S, Yin B *et al.* Impedance spectroscopic study of corrosion inhibition of copper by surfactants in the acidic solutions. *Corros Sci* 2003;**45**:867–82.
[87] Banerjee G, Malhotra SN. Contribution to adsorption of aromatic amines on mild steel surface from HCl solutions by impedance, UV, and Raman spectroscopy. *Corrosion* 1992;**48**:10–5.
[88] Lebrini M, Lagrenee M, Vezin H *et al.* Electrochemical and quantum chemical studies of new thiadiazole derivatives adsorption on mild steel in normal hydrochloric acid medium. *Corros Sci* 2005;**47**:485–505.
[89] Deng S, Li X. Inhibition by *Jasminum nudiflorum* Lindl. Leaves extract of the corrosion of aluminium in HCl solution. *Corros Sci* 2012;**64**:253–62.
[90] Karthik G, Sundaravadivelu M, Rajkumar P. Corrosion inhibition and adsorption properties of pharmaceutically active compound esomeprazole on mild steel in hydrochloric acid solution. *Res Chem Intermed* 2015;**41**:1543–58.
[91] Farsak M, Kelesand H, Keles M. A new corrosion inhibitor for protection of low carbon steel in HCl solution. *Corros Sci* 2015;**98**:223–32.
[92] Alamiery AA. Study of corrosion behavior of N'-(2-(2-oxomethylpyrrol-1-yl) ethyl) piperidine for mild steel in the acid environment. *Biointerface Research in Applied Chemistry* 2021;**12**:3638–46.
[93] Alamiery AA. Investigations on corrosion inhibitory effect of newly quinoline derivative on mild steel in HCl solution complemented with antibacterial studies. *Biointerface Research in Applied Chemistry* 2021;**12**:1561–8.
[94] Al-Amiery AA. Anti-corrosion performance of 2-isonicotinoyl-n-phenylhydrazinecarbothioamide for mild steel hydrochloric acid solution: insights from experimental measurements and quantum chemical calculations. *Surf Rev Lett* 2021;**28**:2050058.
[95] Zinad DS, Salim RD, Betti N *et al.* Comparative investigations of the corrosion inhibition efficiency of a 1-phenyl-2-(1-phenylethylidene)hydrazine and its analog against mild steel corrosion in hydrochloric acid solution. *Progress in Color, Colorants and Coatings* 2021;**15**:53–63.
[96] Salim RD, Betti N, Hanoon M, Al-Amiery AA. 2-(2,4-Dimethoxybenzylidene)-N-phenylhydrazinecarbothioamide as an efficient corrosion inhibitor for mild steel in acidic environment, progress in color. *Colorants and Coatings* 2021;**15**:45–52.
[97] Al-Amiery AA, Shaker LM, Kadhum AH, Takriff MS. Exploration of furan derivative for application as corrosion inhibitor for mild steel in hydrochloric acid solution: effect of immersion time and temperature on efficiency. *Materials Today: Proceedings* 2021;**42**:2968–73.
[98] Resen AM, Hanoon MM, Alani WK *et al.* Exploration of 8-piperazine-1-ylmethylumbelliferone for application as a corrosion inhibitor for mild steel in hydrochloric acid solution. *Int. J. Corros. Scale Inhib.* 2021;**10**:368–87.
[99] Hashim FG, Salman TA, Al-Baghdadi SB *et al.* Inhibition effect of hydrazine-derived coumarin on a mild steel surface in hydrochloric acid. *Tribologia* 2020;**37**:45–53.
[100] Singh AK, Quraishi MA. The effect of some bis-thiadiazole derivatives on the corrosion of mild steel in hydrochloric acid. *Corros Sci* 2010;**52**:1373–85.
[101] Singh AK, Singh M, Thakur S *et al.* Adsorption study of N (−benzo [d] thiazol-2-yl)-1-(thiophene-2-yl) methanimine at mild steel/aqueous H2SO4 interface. *Surfaces and Interfaces* 2022;**33**:102169.
[102] Chugh B, Singh AK, Thakur S *et al.* Comparative investigation of corrosion-mitigating behavior of thiadiazole-derived bis-Schiff bases for mild steel in acid medium: experimental, theoretical, and surface study. *ACS omega* 2020;**5**:13503–20.